Ultrasonics 99 (2019) 105949

Contents lists available at ScienceDirect

Ultrasonics

journal homepage: www.elsevier.com/locate/ultras

Correction of phase rotation in pulse spectrum method for scanning acoustic microscopy and its application to measurements of cells

Ryo Nagaoka[a,*], Kazuto Kobayashi[b], Mototaka Arakawa[c], Hideyuki Hasegawa[a], Yoshifumi Saijo[d]

[a] Laboratory of Medical Information Sensing, Graduate School of Science and Engineering for Research, University of Toyama, Toyama 930-8555, Japan
[b] Division of Research and Development, Honda Electronics, Co. Ltd., Toyohashi 441-3193, Japan
[c] Department of Medical Ultrasound, Graduate School of Biomedical Engineering, Tohoku University, Sendai 980-8579, Japan
[d] Department of Biomedical Imaging, Graduate School of Biomedical Engineering, Tohoku University, Sendai 980-8579, Japan

ARTICLE INFO

Keywords:
Scanning acoustic microscopy
Wiener filtering
Mechanical properties
Thickness
Cells

ABSTRACT

Scanning acoustic microscopy (SAM) can measure the mechanical properties, such as sound speed, thickness, and density, of biological tissues, by using the pulse spectrum method. However, the estimation method needs to be modified because of increases in the center frequency of acoustic transducers. In this paper, we proposed a new estimation method combining a time-of-flight method by Wiener filtering with the pulse spectrum method. First, an optimal control parameter β for Wiener filter was chosen based on a simulation by k-wave MATLAB toolbox. Setting the thickness of a layer to be 1.95 μm, a bias error between the estimated and true thickness was 0.0016% and the control parameter β was chosen to be 0.01 based on the simulated result and previous research. Next, the thickness of a film sample was measured by the time-of-flight method with Wiener filtering and was compared with an optically-measured thickness to confirm the estimation accuracy. Thickness was estimated to be 18.3 ± 0.025 μm at a center frequency of 120 MHz and agreed with the optically-measured thickness. Finally, the parameter n, the number of phase rotation in Gaussian plane, is calculated from the thickness and sound speed, and the pulse spectrum method with the correction of the parameter n is applied to the cellular measurements. Also, the mechanical properties estimated by the proposed method was compared with these by the conventional method.

1. Introduction

In the 1970s, scanning acoustic microscopy (SAM) has been developed to visualize insides of solid specimens and biological tissues non-destructively in non-contact [1,2]. In the last decade, SAM with a spatial resolution of 1–10 μm was used for the measurements of cells, owing to the development of a high-speed A/D converter and higher frequency transducer with the center frequency of up to 500 MHz [3–5]. In our research group, the high frequency transducers have been manufactured based on a simulation in frequency characteristics [6]. The frequency characteristics of the ultrasonic transducers are shown in Fig. 1. Polyvinylidene fluoride (PVDF) ultrasonic transducer and zinc-oxide (ZnO) ultrasonic transducer are commonly used in frequencies of less than 100 MHz and more than 100 MHz, respectively.

Not limited to the morphological information, the SAM measures mechanical properties, such as sound speed, thickness, and acoustic impedance [7–10]. Fig. 2(a) shows the schematic of a measurement condition. The echo signals reflected from a reference, the top surface of a sample, and the boundary between the sample and reference are defined as S_{ref}, S_s, and S_d, respectively. A slide glass or Petri dish is typically used as the reference. Time-of-flight method is the simplest measurement technique [7,8], and is easily implemented by searching the delay times of the received signals to estimate the mechanical properties. However, the received signals cannot be separated into the signal from the boundary S_d and that of the sample surface S_s in the case of the sample with a thickness of less 5 μm due to an axial resolution of approximately 10 μm. For this reason, a pulse spectrum method, utilizing the interference obtained by normalizing the signals S_d and S_s by the reference signal S_{ref} in Fourier domain (Fig. 2(b)), has been developed [9]. Alternatively, the mechanical properties were estimated after separating the received signals into the signal of interest and noise by using autoregression (AR) method [10]. Also, X. Zhao et al. proposed the Multi-Layer Phase Analysis (MLPA) method by focusing $V(z)$ curves [11,12]. The MLPA was combined with atomic force microscope (AFM) to reveal changes in the elastic properties of the cells [13].

In pulse spectrum method, a parameter, which corresponds to the

* Corresponding author.
E-mail address: nryo@eng.u-toyama.ac.jp (R. Nagaoka).

https://doi.org/10.1016/j.ultras.2019.105949
Received 28 March 2018; Received in revised form 21 June 2019; Accepted 21 June 2019
Available online 29 June 2019
0041-624X/

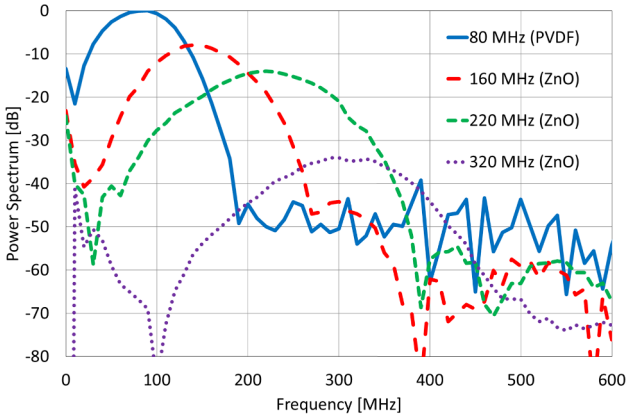

Fig. 1. Frequency characteristics of transducers for acoustic microscopy. Abbreviations of PVDF and ZnO express Polyvinylidene fluoride (PVDF) and zinc-oxide (ZnO) ultrasonic transducer, respectively.

number of rotations in the Gaussian plane, needs to be carefully chosen, and an incorrect estimation of the parameter n leads to the critical error in the calculation of the thickness and sound velocity. In previous research [9], because the bandwidth of the transducer ranged up to around 100 MHz and the thickness of the sample was assumed to be 6–10 μm, the parameter n was assumed to be 1. However, in the present study, the upper frequency has reached to around 500 MHz as shown in Fig. 1. Fig. 3 shows the calculated interferences in the frequency domain [14] in cases of the samples with different sound speeds of 1450, 1500, 1550, 1600, and 1650 m/s. The parameters used in the calculation was as follows: The sound speeds of water and the reference are 1483, and 2340 m/s, respectively. The densities of water, the sample, and reference are 998, 1048, and 1050 kg/m^3, respectively. The interferences with the thicknesses of 2, 4, 6, 8, and 10 μm are shown in Fig. 3(a)–(e), respectively. The maxima and minima of the intensities changed depending on the sample's mechanical properties, and the number of the rotation n is totally different even in the same frequency range. Hence, the prior information in the phase rotation will improve the estimation accuracy of the pulse spectrum method.

In this paper, we propose a new pulse spectrum method with the correction of the parameter n. The parameter n is calculated by the time-of-flight based method by Wiener filtering [15,16]. The spatial resolution can be improved by employing the Wiener filter for the received signals, and the thickness and sound speed are measured by applying the time-of-flight method to the filtered signals. The mechanical properties can then be estimated by the conventional pulse spectrum method with the correction of the parameter n. First, an optimal control parameter β for Wiener filter is chosen based on a simulation. Next, the thickness of a film is measured by the time-of-flight method with Wiener filtering and is compared with an optically-measured thickness to show the estimation accuracy. Finally, the thickness and sound speed of cells is estimated by the time-of-flight method with Wiener filtering. The parameter n is then calculated from the thickness and sound speed, and the pulse spectrum method with the correction of the parameter n is applied to the cellular measurements. Also, the mechanical properties estimated by proposed pulse spectrum method is compared with those by the conventional method.

2. Materials and methods

2.1. Simulation

The optimal control parameter β for Wiener filter was investigated based on the simulation by k-wave MATLAB toolbox [17]. The parameters used for the simulation is shown in Table 2. A substrate was located at the depth of 0.2875 mm corresponding to the focal length of the transducer in the experiment. The grid size in the lateral and depth directions corresponds to a one-eighth of the wavelength. In this condition, the simulation was performed to obtain a reference signal. Next, the region of a cell layer was set on the substrate and the thickness was 1.95 μm, which was less than a half of the wavelength. The simulation was performed to obtain a signal from the cell, a signal of interest. A white noise was added to the signals to adjust a signal noise ratio (SNR) to 60 dB. The thickness was estimated from the simulated signals by using the time-of-flight method with Wiener filtering. A bias error between the estimated and true thickness was also calculated by changing the control parameter β with an interval of 0.0001 from 0.001 to 0.5. The control parameter β at the minimum bias error was used in following experiments.

2.2. Measurement system

A commercially available scanning acoustic microscopy (AMS-50SI, Honda Electronics Co., Ltd, Toyohashi, Japan) [6] was used in the

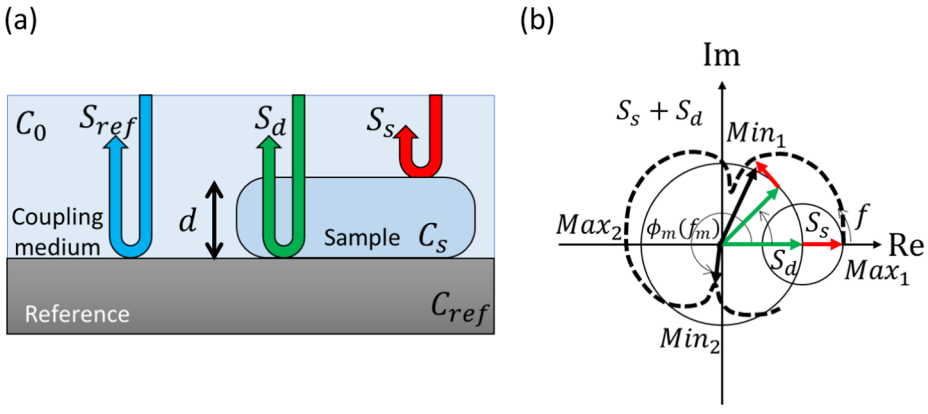

Fig. 2. (a) Schematic of measurement condition. The echo signals reflected from a reference, the top surface of the sample, and a boundary between the reference and sample are defined as S_{ref}, S_s, and S_d, respectively. (b) Interference between the signals of s_d and s_s in complex plane.

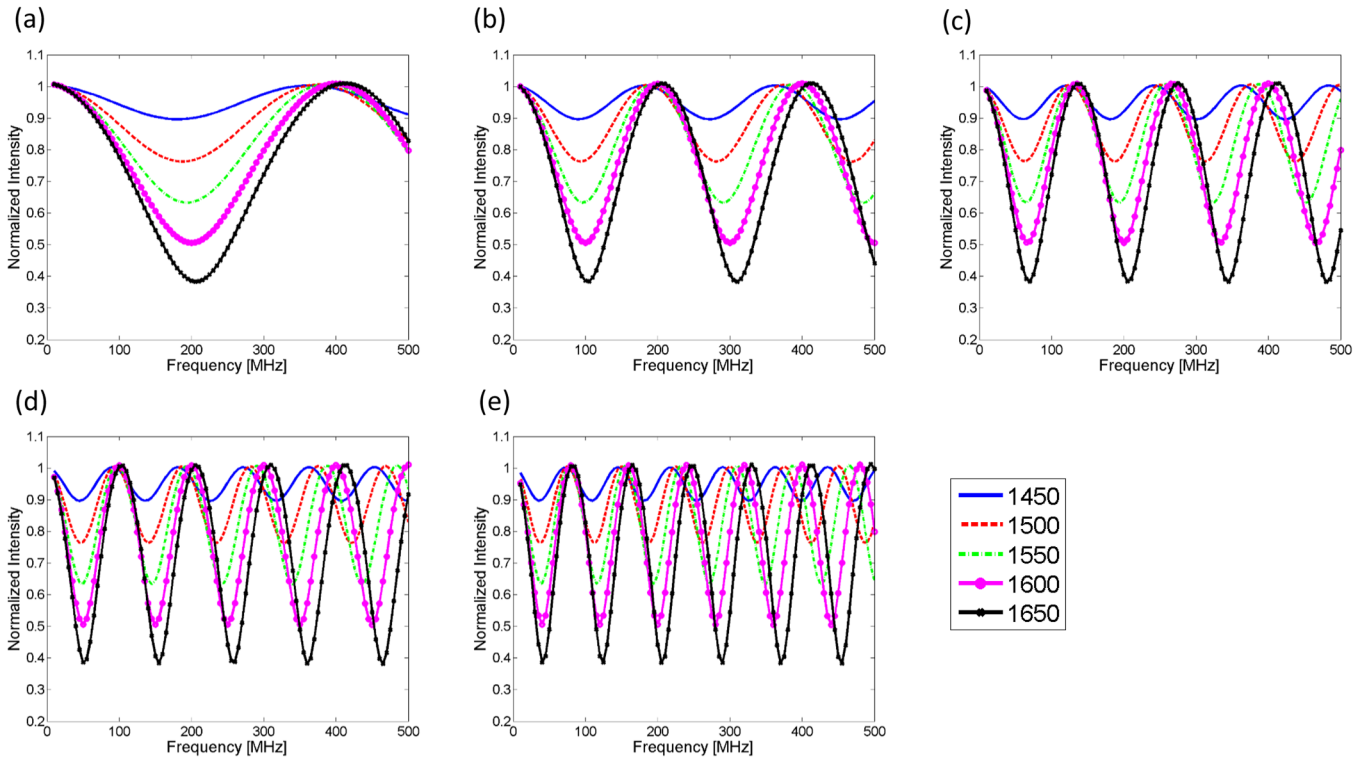

Fig. 3. Interference in the frequency domain in the case of the difference sound speed samples with 1450, 1500, 1550, 1600, and 1650 m/s. Sound speeds of water, and reference are 1483, and 2340 m/s, respectively. Densities of water, sample, and reference are 998, 1048, and 1050 kg/m^3, respectively. The interferences are shown with the thicknesses of (a) 2, (b) 4, (c) 6, (d) 8, and (a) 10 μm, respectively.

following experiments. An acoustic wave was transmitted and received by the same transducer. A frequency of an excitation signal driven by an electric pulse ranged from 10 to 500 MHz, and the bandwidth of a signal receiver was from DC to 700 MHz. The received signals were acquired with a sampling frequency of 2 GHz (8 bits), and the measurement at each point was performed eight times and averaged in order to reduce noise components. Distilled water was used as coupling medium between the film sample and transducer in the film measurements, and saline solution was used in the measurement of cells. Two-dimensional measurements were conducted in 4-μm steps for an area of $1.2 \times 1.2\,\mathrm{mm}^2$ in the former experiment, and in 1-μm steps for an area of $0.3 \times 0.3\,\mathrm{mm}^2$ in the latter experiment.

In this paper, four different transducers as shown in Table 1 were employed. Transducer #1 corresponded to a concave PVDF transducer (Toray Engineering Co., Ltd, Tokyo, Japan) with a center frequency of 80 MHz. The radius of aperture and focal length were 1.2 and 1.5 mm, respectively. The other three transducers #2–#4 were developed by our research groups based on the simulated design [6]. An acoustic lens and a piezoelectric material of ZnO are mainly used in a frequency of more than 100 MHz. ZnO transducer is constructed on the plane surface of the rod having the acoustic lens. Z-cut sapphire single crystal with a sound speed of 11,217 m/s is typically chosen as the rod to achieve a narrow acoustic focused beam. Table 1 shows the detailed information on the geometric properties of ZnO transducers.

2.3. Time-of-flight method

Defining the delay time of the signals S_{ref}, S_s, and S_d as t_0, t_1, and t_2, respectively, the thickness d of the sample can be expressed as

$$d = \frac{t_0 - t_1}{2} c_0, \tag{1}$$

where c_0 is the sound speed of the coupling medium. Also, the sound speed c_s can be expressed as

$$c_s = \left(\frac{t_2 - t_0}{2d} + \frac{1}{c_0} \right)^{-1}. \tag{2}$$

2.4. Pulse spectrum method

In the interference, maxima ($Max_{\#}$) alternated with minima ($Min_{\#}$) repeatedly in the Gaussian plane as shown in Fig. 2(b). The length of

Table 1
Geometric and frequency properties of four transducers.

Transducer #	Material	Center frequency [MHz]	Theoretical lateral resolution [μm]	Radius of aperture [mm]	Focal length [mm]
1	P(VDF-TrFE)	80	23.4	1.2	1.5
2	ZnO	160	8.3	1.0	1.15
3	ZnO	220	6.0	0.5	0.575
4	ZnO	320	4.2	0.25	0.2875

Table 2
Parameters for simulation.

Focused ultrasonic transducer		
Center frequency [MHz]		300
Bandwidth [%]		100
Number of pulse cycle		3
Focal length [mm]		0.2875
Opening angle [°]		90
Mechanical properties		
Material	Sound speed [m/s]	Density [kg/m^3]
Water	1500	1000
Substrate (polystyrene)	2340	1040
Cell (nucleus)	1650	1030
Grid size		
Spatial interval along axial direction [μm]		0.975
Spatial interval along lateral direction [μm]		0.975
Value of Courant-Friedrichs-Lewy (CFL)		0.05

arrows corresponds to the normalized intensity of the interference and its angle corresponds to a phase ϕ. Let $f_{Max_\#}$ and $f_{Min_\#}$ denote frequencies at the maxima and minima, respectively. The corresponding phase angles $\phi_{Max_\#}$ and $\phi_{Min_\#}$ at the maxima and minima are expressed as follows,

$$2\pi f_{Min_\#} \times \frac{2d}{c_0} = \phi_{Min_\#} + (2n-1)\pi, \tag{3}$$

and

$$2\pi f_{Max_\#} \times \frac{2d}{c_0} = \phi_{Max_\#} + 2n\pi, \tag{4}$$

where n is a non-negative integer, and d is the thickness of the sample. Focusing on the minima, the phase angle $\phi_{Min_\#}$ can be expressed by

$$2\pi f_{Min_\#} \times 2d\left(\frac{1}{c_0} - \frac{1}{c_s}\right) = \phi_{Min_\#}. \tag{5}$$

The phase angle is the lag between the acoustic wave passing through the thickness $2d$ with sound speed c_s and through the corresponding thickness with the sound speedc_0. From the Eqs. (3) and (5), the thickness at the minimum $Min_\#$ can be given by

$$d = \{\phi_{Min_\#} + (2n-1)\pi\} \times \frac{c_0}{4\pi f_{Min_\#}}. \tag{6}$$

Then, the sound speed c_s can be written as

$$c_s = \left(\frac{1}{c_0} - \frac{\phi_{Min_\#}}{4\pi f_{Min_\#} d}\right)^{-1}. \tag{7}$$

2.5. Wiener filtering and the estimation method of thickness and sound speed by time-of-flight based method

The Wiener filter $M(\omega)$ restores the bandwidth of the received

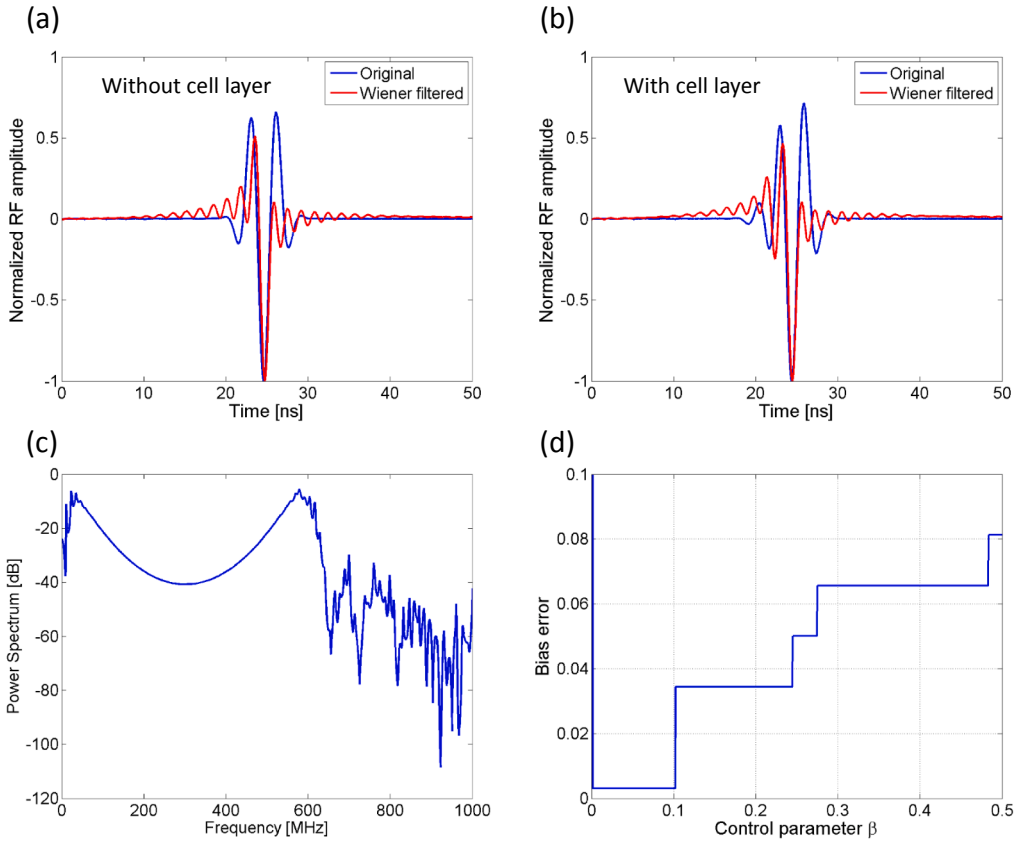

Fig. 4. Simulation results: Comparisons between the original and Wiener filtered signals (a) without and (b) with cell layer. (c) Power spectrum of Wiener filter. (d) Bias error between the true and estimated thicknesses.

signals degraded by the transducer characteristics and attenuation in coupling media [15,16] and is expressed in the Fourier domain as

$$M(\omega) = \frac{H^*(\omega)}{|H(\omega)|^2 + \beta\frac{N(\omega)}{S(\omega)}}, \tag{8}$$

where $H(\omega)$, β, $N(\omega)$, and $S(\omega)$ are an impulse response, the optimal control parameter, a noise level, and a signal revel, respectively. The impulse response includes not only the characteristics of the ultrasonic transducer but also the frequency dependent attenuation in coupling media. The frequency characteristic of the noise level $N(\omega)$ was obtained by the measurement without the samples. The spectrum of the signal level $S(\omega)$ was calculated by averaging the signals reflected from the reference region. Also, the signal level $S(\omega)$ was employed as the impulse response $H(\omega)$. The region where the intensities of the reflected signals were highest was chosen as the reference region. Let $rs(t)$ be the reflected signal, and the relationship is written as

$$rs(t) = s_d(t) + s_s(t). \tag{9}$$

Wiener filtering in the frequency domain can be expressed by

$$rs_F(t) = IFT[rs(\omega) \times M(\omega)], \tag{10}$$

where $rs_F(t)$ and $IFT[\cdot]$ are the Wiener filtered signals, and inverse Fourier transform, respectively. The delay times corresponding the closest and furthest peaks against the transducer surface in the sample region were defined as t_1 and t_2, respectively. Also, the delay time at the peak of the envelope in the reference region corresponded to t_0. The thickness and sound speed were calculated by plugging these delay times in the Eqs. (1) and (2).

2.6. Pulse spectrum method with the correction of parameter n

Eqs. (6) and (7) are rewritten by the frequency f_m and phase ϕ_m at the extrema as follows,

$$d = \{\phi_m + n\pi\} \times \frac{c_0}{4\pi f_m}, \tag{11}$$

$$c_s = \left(\frac{1}{c_0} - \frac{\phi_m}{4\pi f_m d}\right)^{-1}. \tag{12}$$

From these two equations, the parameter n can be obtained by

$$n = round\left(\frac{4df_m}{c_s}\right), \tag{13}$$

where $round(*)$ is a rounding process, down to the nearest integer. The thickness and sound speed by the time-of-flight method with Wiener filtering was used for the calculation of n. Also, the frequency f_m was assumed to be the center frequency of the transducer. When there was a zero value in the measurement area, which was chosen from the intensity of the C-mode images, the value was interpolated from the parameter at a nearest neighbor position. The pulse spectrum method [9] with the calculated parameter n was then applied to the received signals.

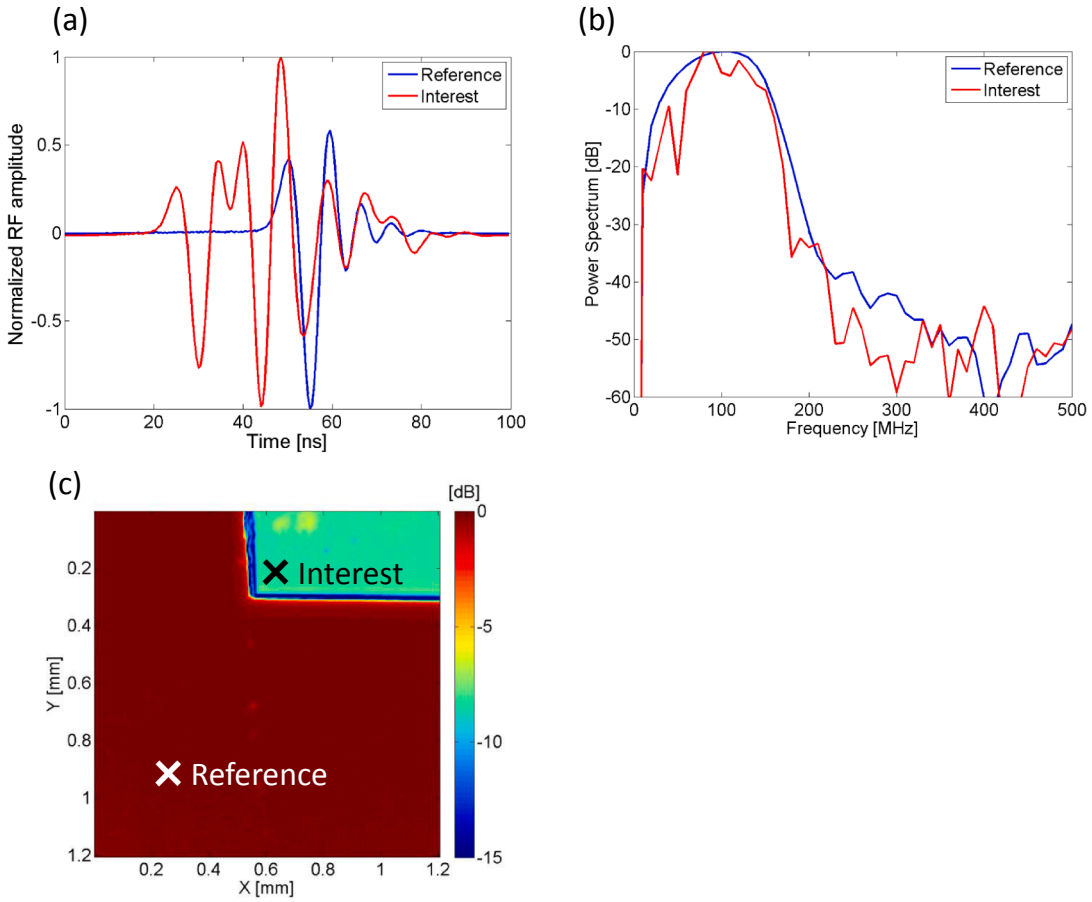

Fig. 5. Measurement results of the film sample by using the transducer with the center frequency of 80 MHz. (a) Comparison between signals reflected from interest point and reference points, (b) the power spectra, and (c) C-mode image of the film sample.

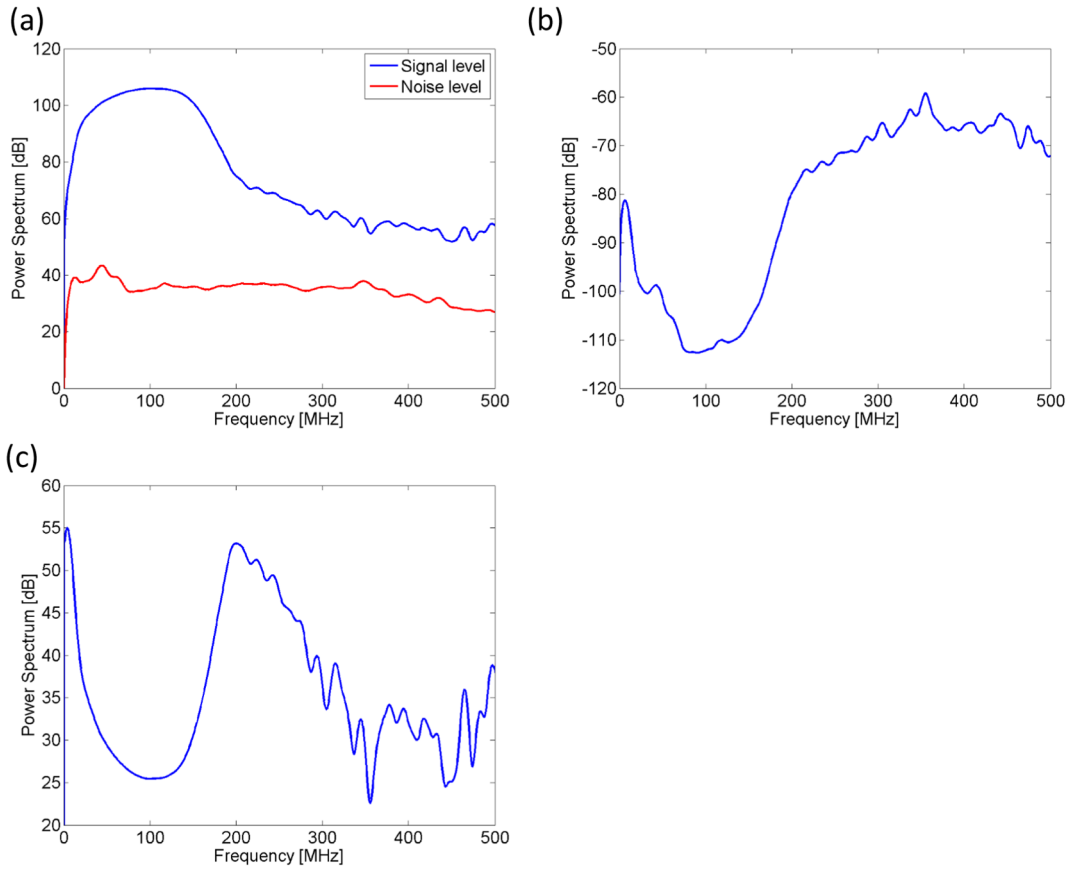

Fig. 6. (a) Signal and noise levels of the transducer with the center frequency of 80 MHz, (b) Noise-signal level, and (c) calculated Wiener filter.

2.7. Verification experiments by using polyimide film

In this experiment, the thickness of the film was estimated by using the time-of-flight method with Wiener filtering. The sample was made by attaching polyimide film (Kapton 50H (12.5 μm), Du Pont-Toray Co., Ltd., Tokyo, Japan) on the glass plate with bonding agent. As a comparison, the thickness was measured by a 3D laser scanning confocal microscope (VK-X250, Keyence Corp., Osaka, Tokyo). Then, the results by employing four different transducers were compared with the optically measured thickness in the same region.

2.8. Preparation of cells and the experiment

MG-63 human osteosarcoma lines were cultured on a polystyrene dish (100 mm diameter) coated in Eagle's minimal essential medium with nonessential amino acids and mixed solution containing 10% fetal bovine serum (FBS) and 1% antibiotics and kept at 37 °C in 5% CO_2. Before the SAM measurement, the culture medium was replaced by saline. First, the cells were measured to estimate the distribution of the thickness, sound speed, and parameter n by using the time-of-flight method with Wiener filtering. Next, the conventional and proposed pulse spectrum method were applied to the measured signals. Also, by assuming the density of the cells to 1030 kg/m^3, the acoustic impedance was calculated. In the conventional pulse spectrum method, the parameter n was assumed to be 1. Finally, the results were compared. In this cellular experiment, only transducer #4 was used for the measurement due to the limited spatial resolution and the cellular size. The measurements were treated in accordance with guidelines approved by the committee on experiments of Tohoku University.

3. Results

3.1. Simulation results

Fig. 4(a) and (b) show comparison between the original and Wiener filtered signals without/with the cell layer, respectively. Fig. 4(c) shows the power spectrum of the designed Wiener filter. The Wiener filtering improved the pulse width, and the signal of interest could be separated into the signal from the substrate and cell layer. The time-of-flight method was applied to the Wiener filtered signals to estimate the layer thickness. A minimum bias error of 0.0016% was obtained in a range from 0.005 to 0.1 as shown in Fig. 4(d). The control parameter β was chosen to be 0.01 based on the simulated result and the previous papers [15,16].

3.2. Results of the film sample

Fig. 5 shows the results of the film sample by using the transducer with a center frequency of 80 MHz. Fig. 5(a)–(c) show a comparison between signals reflected from interest and reference points, the power spectra, and the C-mode image of the film sample, respectively. A red[1] line corresponds to the signals from the interest point, and a blue one corresponds to that from the reference point. As seen from Fig. 5(a), the original signals reflected from the interest point cannot be separated into the signalsS_d and S_s. Fig. 6(a) shows the signal level $S(\omega)$ (blue line) and noise level $N(\omega)$ (red line) of the transducer, and Fig. 6(b) shows the noise-signal level $N(\omega)/S(\omega)$. The Wiener filter was calculated from

[1] For interpretation of color in Figs. 5-7, 13 and 17, the reader is referred to the web version of this article.

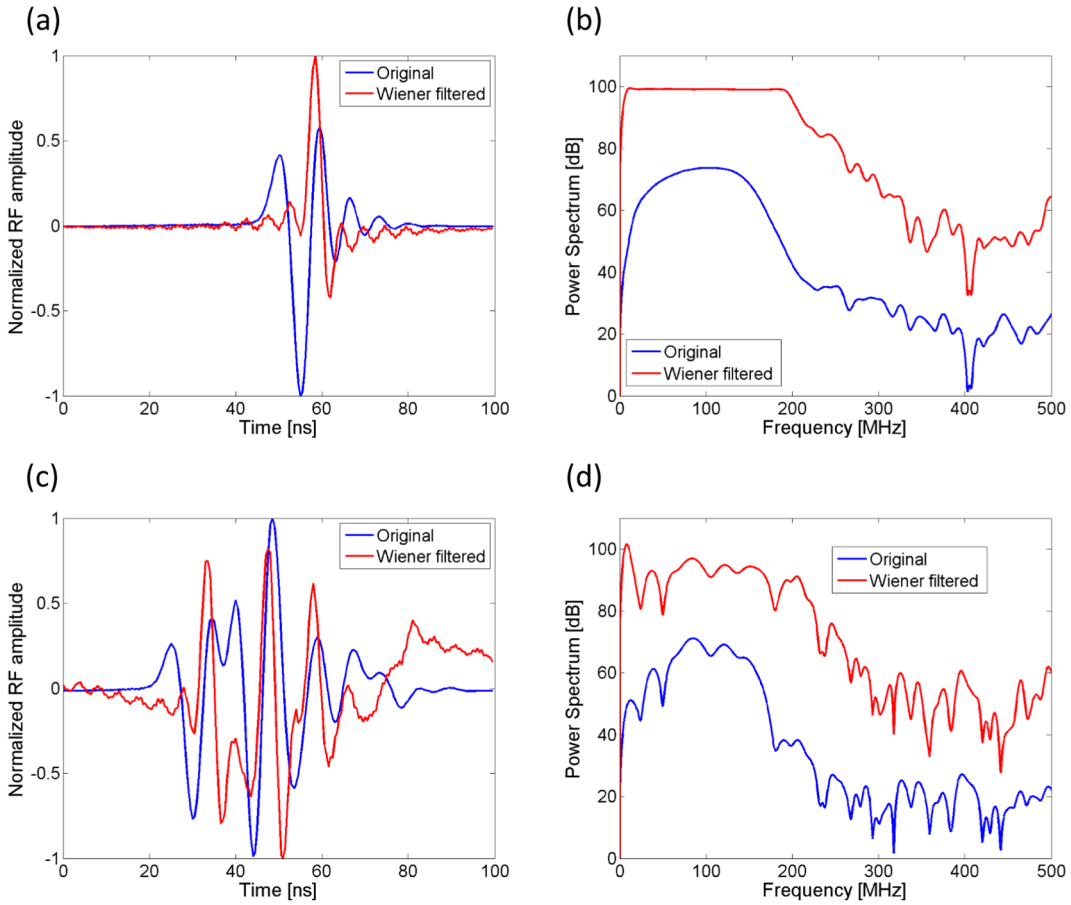

Fig. 7. Comparisons between the original and Wiener filtered signals. (a) The signals reflected from the reference point (the glass region), and (b) the power spectra. (c) The signals reflected from the interest point (the film region), and (d) the power spectra.

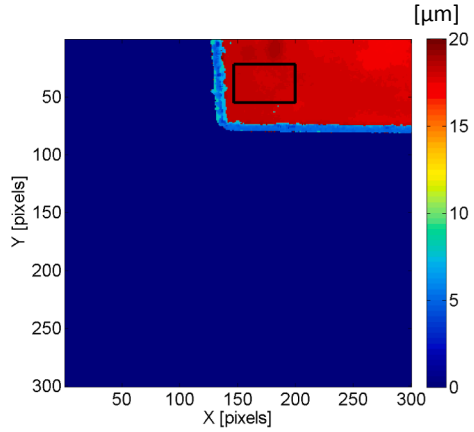

Fig. 8. Thickness 2D map estimated by the time-of-flight method with Wiener filtering.

these characteristics as shown in Fig. 6(c). Fig. 7 shows the comparisons between the original (blue line) and Wiener filtered signals (red line). Fig. 7(a) and (b) show the signals from the reference point and the power spectra, respectively. Similarly, Fig. 7(c) and (d) show the signals from the interest point and the power spectra, respectively. As seen from Fig. 7(b), the power spectrum could be restored to be flat in the range between 10 MHz and 200 MHz by the Wiener filter. Additionally, the pulse length in the time domain can be clearly improved as shown in Fig. 7(a) and (c). Fig. 8 shows the thickness 2D map estimated by the proposed time-of-flight method. The thickness in a ROI surrounded by a black square was 18.20 ± 0.025 μm.

Fig. 9 shows the measurement results of the film sample by the 3D laser scanning confocal microscope. Fig. 9(a)–(c) show the optical image of the film sample, the 3D thickness distribution, and the thickness profile on the line in Fig. 9(a), respectively. The maximum and minimum thicknesses of the sample were 18.858, and 17.985 μm, respectively.

Fig. 10 shows the comparison of the averaged values (dots) by the acoustic method with the maximum and minimum thicknesses measured by the optical method. Error bars correspond to standard deviations. The result concluded that the time-of-flight based method with the Wiener filter can separate the interfered signals into the two signals even in the situation where the thickness of the sample was less than the ultrasonic wavelength.

3.3. Measurement results of the cells

Fig. 11 shows the results of cells. Fig. 11(a) shows the C-mode image of the cells by using the transducer with the center frequency of 320 MHz in the scanning region of 1.2 × 1.2 mm^2. Fig. 11(b) shows the C-mode image of cells in the scanning region of 0.3 × 0.3 mm^2

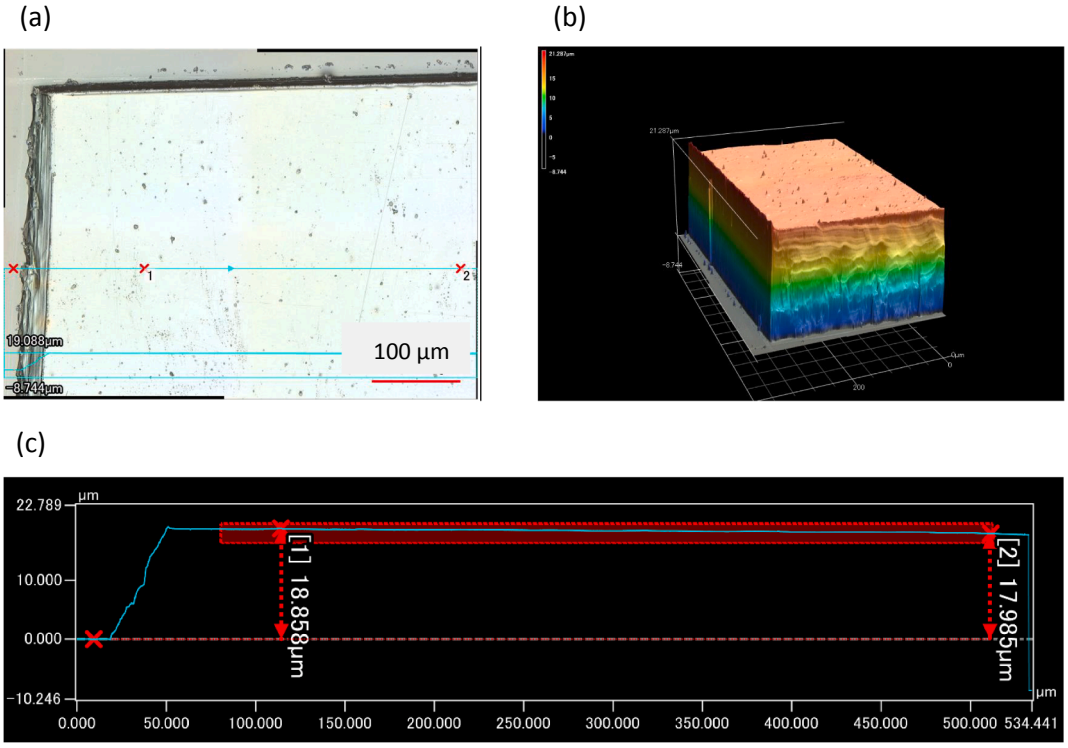

Fig. 9. Measurement results by 3D laser scanning confocal microscope (VK-X250, Keyence Corp.) (a) Optical image of film sample, (b) 3D thickness information of the sample, and (c) thickness profile on the line in (a): Maximum: 18.858 µm, and Minimum: 17.985 µm.

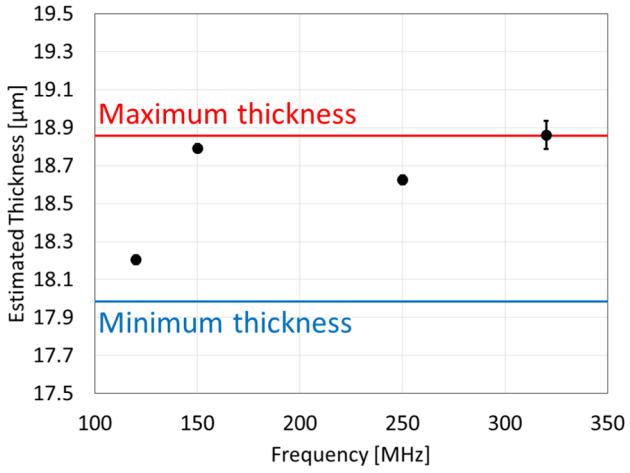

Fig. 10. Comparison of the averaged thickness by the acoustic method with the maximum and minimum thicknesses measured by the optical method. Error bars correspond to the standard deviations.

corresponding to a red square in Fig. 11(a). Fig. 11(c) shows the optical image of the cells. By focusing on the dot line in Fig. 11(b), the B-mode image of the single cell was obtained as shown in Fig. 12. Fig. 12(a) shows the original B-mode image of the cell, and Fig. 12(b) shows the Wiener filtered B-mode image. As seen from Fig. 12, the pulse length of the Wiener filtered signals could be reduced to less than half, and the axial spatial resolution of the B-mode image was improved significantly. The signals from the surface of the cell could also be clearly identified. Fig. 13(a) and (b) show the thickness map and sound speed map of the cells estimated by using the time-of-flight method with Wiener filtering, respectively. Fig. 13(c) shows the parameter n map calculated from the estimated thickness and sound speed. A thickness of approximately 4 µm was estimated in the center region corresponding to a nucleus (yellow region). The estimated thickness almost agreed with the B-mode image. Meanwhile, the thickness in the cytoskeleton region surrounding the nucleus was thinner and estimated to be 2 µm. The measured thickness and sound velocity were in the same extent that was reported in previous papers [5].

Fig. 14(a)–(c) show the estimated distribution of the thickness, sound speed, and acoustic impedance by the corrected pulse spectrum method, respectively. Also, Fig. 14(d)–(f) show the estimated distribution of the thickness, sound speed, and acoustic impedance by the conventional pulse spectrum method, respectively. Fig. 15(a) and (b) show the comparison of the thickness and sound speed along dot lines as shown in Fig. 14. In Fig. 15(a), the thickness by the conventional method was lower than that by the corrected method, especially in the nucleus. This difference was attributable to the false parameter n of 1 in the conventional method. On the other hand, the parameter n was estimated to be 2 by the proposed method, and the thickness by the corrected method shows the same tendency to the result by the time-of-flight method.

4. Discussion

The three signals were observed in Fig. 7(c), and it's likely that the central signal corresponds to the echo signal from the boundary

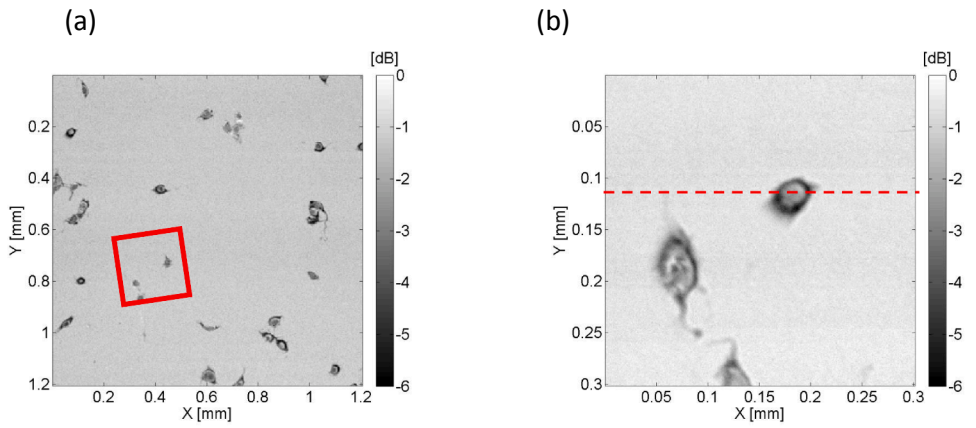

Fig. 11. Measurement results of the cells. (a) C-mode image of cells by using the transducer with the center frequency of 320 MHz in the scanning region of $1.2 \times 1.2\,mm^2$, (b) C-mode image of cells in the scanning region of $0.3 \times 0.3\,mm^2$ corresponding to the red squared area in (a). (c) The optical image of the cells. (For interpretation of the references to color in this figure legend, the reader is referred to the web version of this article.)

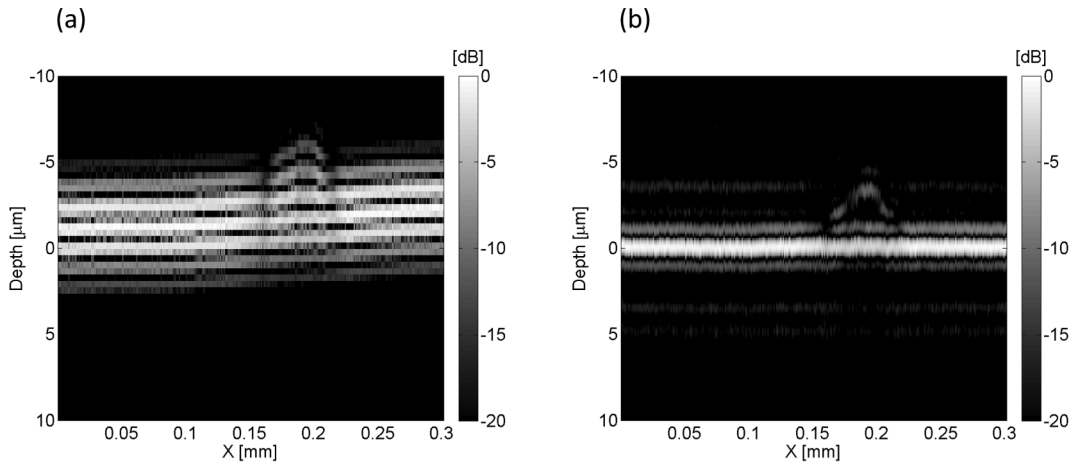

Fig. 12. (a) Original B-mode image, and (b) Wiener filtered B-mode image of the cells along the dot line as shown in Fig. 11 (b).

between the film and layer of bonding agent. The time difference between the first and second peaks was about 13 ns, and the thickness of the film layer was calculated to be 14.3 µm by assuming its sound speed as 2200 m/s. A difference in the thicknesses was caused by an error in the assumed sound speed or the characteristics of the water-absorbency. In this verification experiment, the optical measurement was performed after the film sample was kept in the water during the duration equal to that of the acoustic measurement to minimize an influence by the water-absorbency.

The parameter n corresponds to the number of rotations in the Gaussian plane. Hence, when the ultrasonic transducer has the wide bandwidth from DC to the interested frequency, the number of the rotation can be calculated by applying an unwrapped process to the phase of the normalized signals. However, the limited bandwidth complicates the calculation of the number n. Fig. 16 shows the comparison of the unwrapped phase and phase with the correction of the parameter n when focusing on the signal from the nucleus. In this case, the unwrapping process cannot work well due to the low SNR in a frequency range of less than 150 MHz.

A difference of 1 in the parameter n causes the fatal errors in the estimation. From the Eq. (11), the error value Δd in the thickness can be calculated to be 1.235 µm by assuming the frequency f_m at the extrema

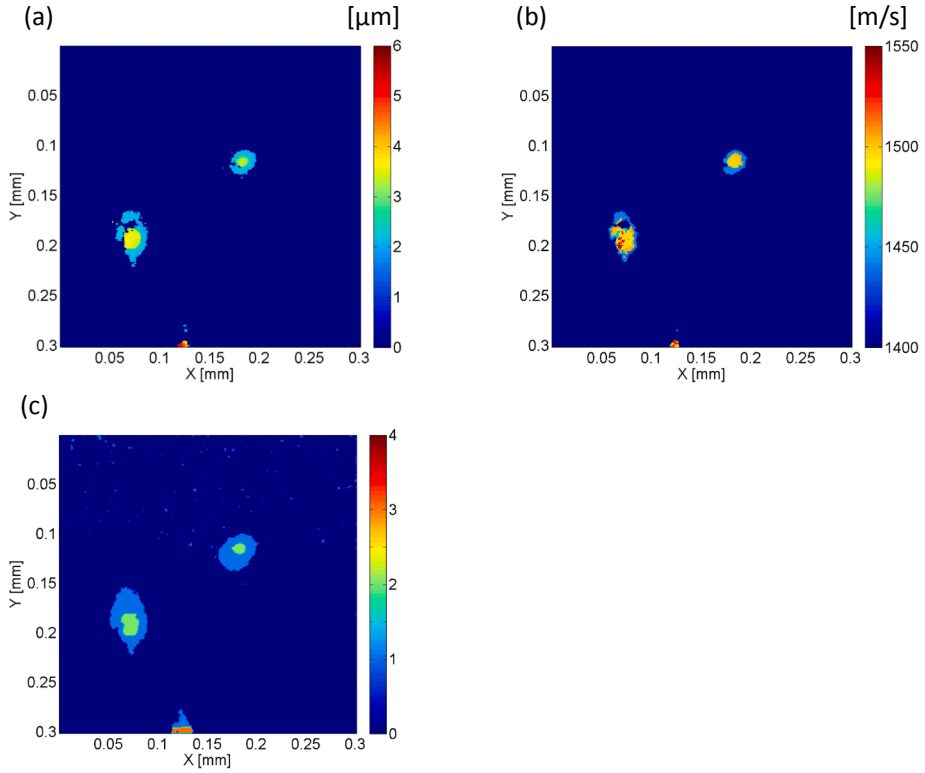

Fig. 13. (a) Thickness map, and (b) sound speed map of the cells estimated by using the time-of-flight method with Wiener filtering. (c) Parameter n map calculated from the thickness and sound speed.

assumed as 300 MHz. Subsequently, the error in the thickness leads to a further error in the calculation of the sound speed. In this case, the error Δc_s reaches to 93.2 m/s by calculating from the Eq. (12). This is supported by the results as shown in Fig. 15.

By focusing on the signal from the nucleus of the cell in Fig. 11(b), Fig. 17 shows the comparison of the power spectrum estimated from the thickness and sound speed (blue line) with the measured one (red line) in the Fourier domain. The estimated interference was calculated from

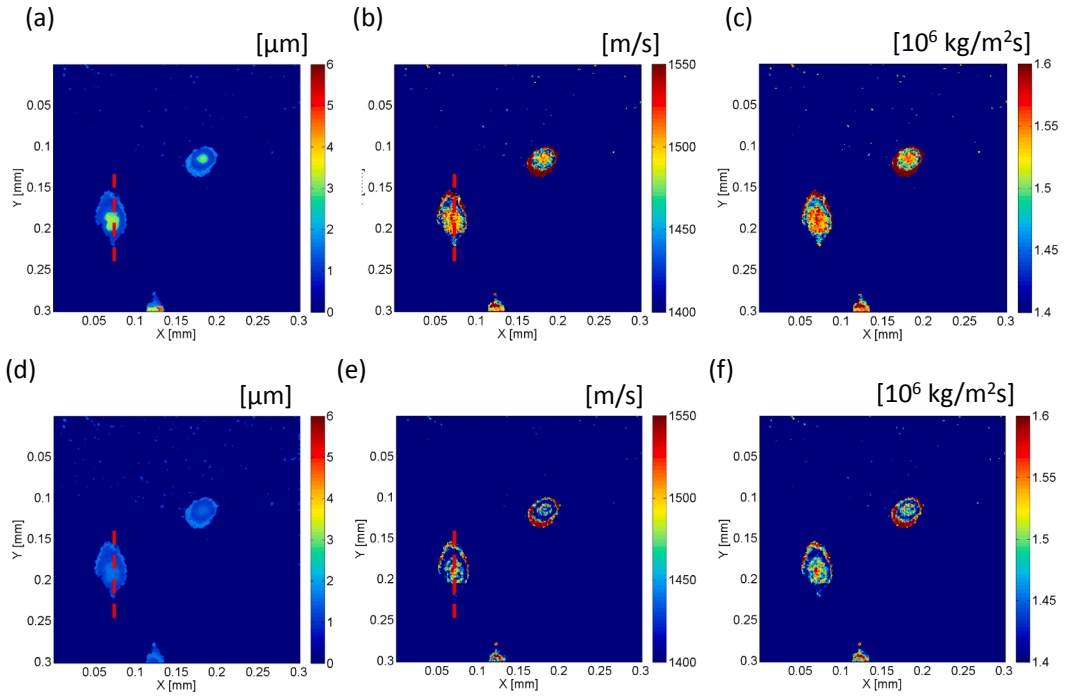

Fig. 14. Estimated distribution of (a) thickness, (b) sound speed, and (c) acoustic impedance by the corrected pulse spectrum method. Estimated distribution of (d) thickness, (e) sound speed, and (f) acoustic impedance by the conventional pulse spectrum method.

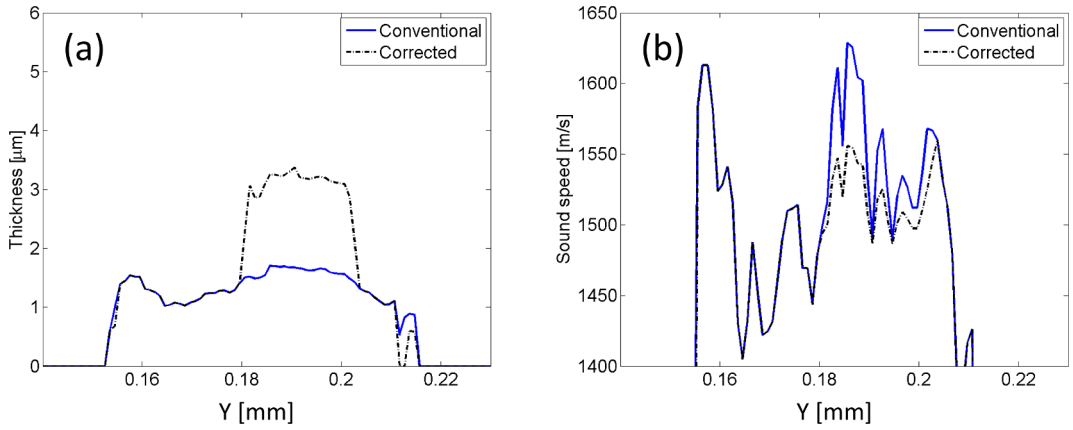

Fig. 15. Comparison of (a) thickness and (b) sound speed along dot lines as shown in Fig. 14.

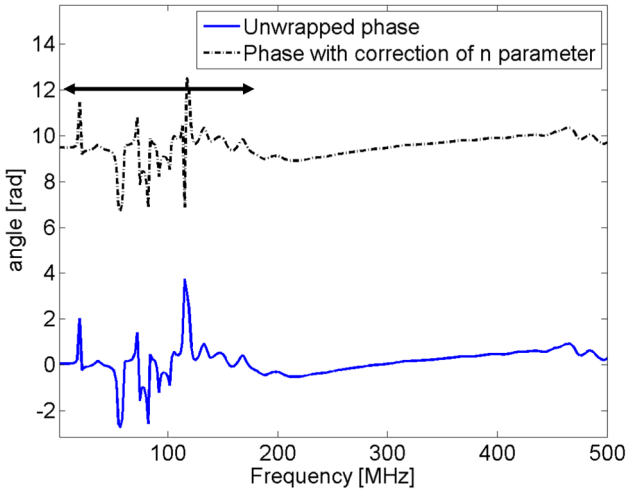

Fig. 16. Comparison of unwrapped phase and phase with correction of parameter *n*.

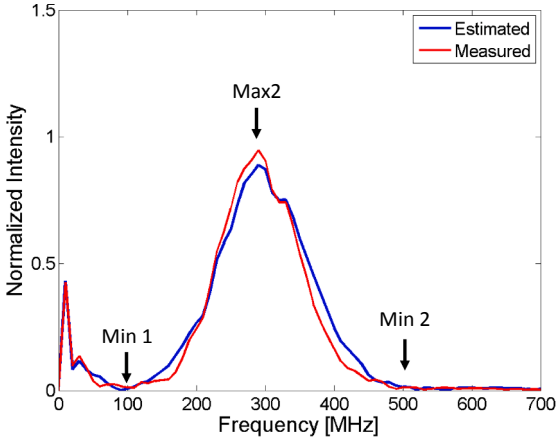

Fig. 17. Comparison of the interference calculated by the estimated thickness and sound speed with the measured interference in the frequency domain.

the prior information based on a simple transmission line model which takes the multi-reflection into consideration [18]. Also, the measured signal was calculated by normalizing the frequency spectrum of the signal of interest with that of the reference signal. The estimated interference well conformed to the measured one. The information on both the minima and maxima in advance will improve the estimation accuracy on the pulse spectrum method.

5. Conclusions

In this paper, we proposed a pulse spectrum method with the correction of the parameter *n*. The parameter *n* was calculated from the thickness and sound speed obtained by the time-of-flight based method. First, setting the thickness of the layer to be 1.95 μm in the simulation, the bias error between the estimated and true thickness was 0.0016%. Next, the thickness of the film sample was estimated by applying the time-of-flight method to the Wiener filtered signals. The thickness was estimated to be 18.3 ± 0.025 μm at a center frequency of 120 MHz and agreed with the optically-measured thickness. Finally, the proposed method was applied to the cellular measurement. The thicknesses of around 2–6 μm were estimated, and the results were compared with those by the conventional method.

In future work, a relationship on the frequency dispersion would be estimated to reveal the mechanical property of viscosity in the cells. We believe this development must be useful for basic studies on the micro structures in the cells.

Acknowledgments

This work was supported a JSPS Grant-in-Aid for Young Scientists (Start-up) 16H066190.

We thank Toshihisa Yano, and Yoshihiro Hagiwara for preparation of the cells.

We also would like to thank Mitsuhiro Fujiwara in Okusonic Corporation for preparation of the film sample.

References

[1] L.W. Korpel, P.R. Kessler, Palermo, acoustic microscope operating at 100 MHz, Nature 232 (1971) 110–111.
[2] R.A. Lemons, C.F. Quate, Acoustic microscopy: biomedical applications, Science 188 (1975) 905–911.
[3] D. Rohrbach, K. Ito, H.O. Lloyd, R.H. Silverman, K. Yoshida, T. Yamaguchi, J. Mamou, Material properties of human ocular tissue at 7-μm resolution, Ultrason. Imag. 39 (5) (2017) 313–325.
[4] K. Ito, Z.-H. Deng, K. Yoshida, J. Mamou, H. Maruyama, T. Yamaguchi, Microscopic acoustic properties analysis of excised rat livers using ultra-high frequency ultrasound, Med. Imag. Tech. 35 (2017) 51–62.
[5] E.M. Strohm, G.J. Czarnota, M.C. Kolios, Quantitative measurements of apoptotic cell properties using acoustic microscopy, IEEE Trans. Ultrason., Ferroelectr., Freq. Contr 57 (2010) 2293–2304.
[6] M. Arakawa, H. Kanai, K. Ishikawa, R. Nagaoka, K. Kobayashi, Y. Saijo, A method for the design of ultrasonic devices for scanning acoustic microscopy using impulsive signals, Ultrasonics 84 (2018) 172–179.
[7] E.C. Weiss, P. Anastasiadis, G. Pilarczyk, R.M. Lemor, P.V. Zinin, Mechanical properties of single cells by high-frequency time-resolved acoustic microscopy, IEEE Trans. Ultrason., Ferroelectr., Freq. Contr 54 (2007) 2257–2271.
[8] M. Arakawa, J. Shikama, K. Yoshida, R. Nagaoka, K. Kobayashi, Y. Saijo, Development of an ultrasonic microscope combined with optical microscope for multiparametric characterization of a single cell, IEEE. Trans. Ultrason., Ferroelectr., Freq. Contr. 62 (2015) 1615–1621.
[9] N. Hozumi, R. Yamashita, C.-K. Lee, M. Nagao, K. Kobayashi, Y. Saijo, M. Tanaka, N. Tanaka, S. Ohtsuki, Time-frequency analysis for pulse driven ultrasonic microscopy for

biological tissue characterization, Ultrasonics 84 (2004) 172–179.
[10] N. Tanaka, K. Kobayashi, N. Hozumi, Y. Saijo, M. Tanaka, S. Ohtsuki, Estimation of echo component in sound speed microscopy for biological tissue, Technical Report US2005-19 (2005) 21–26.
[11] X. Zhao, R. Akhtar, N. Nijenhuis, S.J. Wilkinson, L. Murphy, C. Ballestrem, M.J. Sherratt, R.E.B. Watson, B. Derby, Multi-layer phase analysis: quantifying the elastic properties of soft tissues and live cells with ultra-high frequency scanning, Acoustic Microscopy, IEEE Trans. Ultrason., Ferroelectr., Freq. Contr 59 (4) (2012) 610–620.
[12] L.E. Clarke, J.C. McConnell, M.J. Sherratt, B. Derby, S.M. Richardson, J.A. Hoyland, Growth differentiation factor 6 and transforming growth factor-beta differentially mediate mesenchymal stem cell differentiation, composition, and micromechanical properties of nucleus pulposus constructs, Arthritis Res. Ther. 16 (2) (2014) R67.
[13] N. Nijenhuis, X. Zhao, A. Carisey, C. Ballestrem, B. Derby, Combining AFM and acoustic probes to reveal changes in the elastic stiffness tensor of linving, Biophys. J. 107 (7) (2014) 1502–1512.
[14] G.A.D. Briggs, O.V. Kolosov, Acoustic Microscopy, Oxford University Press, Oxford, 1979.
[15] S. Kageyama, H. Hasegawa, H. Kanai, Increasing bandwidth of ultrasound radio frequency echoes using wiener filter for improvement of accuracy in measurement of intima-media thickness, Jpn. J. Appl. Phys. 52 (2013) 07HF04.
[16] R. Nagaoka, S. Yoshizawa, S.-I. Umemura, Yoshifumi Saijo, Basic study on improvement of axial resolution and suppression of time side lobe by phase-corrected wiener filtering in photoacoustic tomography, Jpn. J. Appl. Phys. 57 (2018) 07LD11.
[17] B.E. Treeby, J. Jaros, D. Rohrbach, B.T. Cox, Modelling elastic wave propagation using the k-Wave MATLAB toolbox, Conf. Proc. IEEE International Ultrasonics Symposium 2014, 2014, pp. 146–149.
[18] K. Yoshida, K. Inoue, S. Irie, M. Jonathan, H. Maruyama, T. Yamaguchi, Acoustic attenuation of rat liver measured by high frequency pulsed ultrasound, Conf. Proc. Ultrason. Electron. 35 (2014) 153–154.